Microsc. Microanal. 19, S5, 202–206, 2013
doi:10.1017/S143192761301266X

Oxidation Mechanism of Nickel Oxide/Carbon Nanotube Composite

Tae-Hoon Kim,[1] Min-Ho Park,[1] Jiho Ryu,[2] and Cheol-Woong Yang[1,*]

[1]*School of Advanced Materials Science and Engineering, Sungkyunkwan University, Suwon, Gyeonggi-do 440-746, South Korea*
[2]*Department of Automobile Development, Ajou Motor College, Boryeong 355-769, Korea*

Abstract: The oxidation mechanism and thermal stability of nickel oxide (NiO)/carbon nanotube (CNT) composites were investigated by examining composites with different NiO contents by thermogravimetric analysis and transmission electron microscopy (TEM). NiO acts as a catalyst in the oxidation of CNT in the composite. CNTs can be oxidized, even in a vacuum, by reducing NiO to nickel at temperatures lower than the normal oxidation temperature of CNTs. This phase transition was confirmed directly by *in situ* heating TEM observations. In air, reduction by CNT occurs simultaneously with reoxidation by gaseous O_2 molecules, and NiO maintains its phase. The thermal stability decreased with increasing NiO content because of defects in the CNT generated by the NiO loading.

Key words: oxidation mechanism, NiO, CNT, composite, *in situ* heating, TEM, TGA, Raman spectroscopy

Introduction

Carbon nanotubes (CNTs), which were first discovered in 1991 by Iijima (1991), have been examined for many applications owing to their excellent properties. CNTs have great potential for a wide range of applications owing to their electrical, thermal, and mechanical properties (Avouris et al., 2007). In addition, the large specific area and small size of the CNTs make them suitable catalyst supports for catalytically active metal and/or metal oxide particles. Therefore, various metal/CNT and metal oxide/CNT composites have been investigated to take full advantage of the multifunctionality of the metal, metal oxide, and CNTs. In the case of metal oxide/CNT composites, CNT can provide a great reaction site because of the large specific area and high electronic conduction path to the metal oxide, which itself has relatively low conductivity (Avouris et al., 2007). Therefore, CNTs are expected to increase the electrochemical utilization of metal oxide. Among the various metal oxides, nickel oxide (NiO) is attractive in view of its low cost, low toxicity, well-defined electrochemical redox activity, and the possibility of enhanced performance through different preparative methods (He et al., 2006). For these reasons, NiO/CNT composites have been studied widely for many possible applications, such as catalysts, electrochromic films, gas sensors, and electrode materials (Xia et al., 2008; Wang et al., 2008; Lota et al., 2011).

For many applications, it is important to understand the oxidation resistance and thermal stability of CNTs in a NiO/CNT composite because they can limit the operation temperature and applicability of the composites. In general, CNTs are oxidized at 600–700°C (Ajayan et al., 1995). On the other hand, catalyst residues, amorphous carbon, and defects can reduce considerably their oxidative stability toward air. In contrast, the oxidative stability can be enhanced by high-temperature vacuum annealing, which produces more graphitic CNTs with a low defect concentration (Osswald et al., 2005; Behler et al., 2006). In addition, in NiO/CNT composites, the oxidation resistance and temperature of CNT can be affected by NiO around the CNT, and the oxidation state of the NiO/CNT composite can affect its characteristics and performance (Li et al., 2004; Aksel & Eder, 2010). Therefore, the oxidation mechanism and thermal stability of NiO/CNT composite should be examined in detail.

In this study, NiO/CNT composites with different NiO contents were prepared using a solution-based method. Thermogravimetric analysis (TGA) in air and N_2 confirmed the NiO loading on CNT and the decrease in oxidation temperature with increasing NiO content. The oxidation mechanism was predicted from these data. Transmission electron microscopy (TEM), with *ex situ* and *in situ* heat treatment, was used to observe the microstructure.

Materials and Methods

NiO/CNT composites were prepared by the thermal decomposition of nickel nitrate on CNTs. Multi-walled carbon nanotubes (MWCNT, M95, Carbon Nano-Material Technology Co. Ltd.) and $N_2NiO_6 \cdot 6H_2O$ with various contents (10, 30, 50 and 80 wt% NiO) were dissolved in ethanol. The samples were heat-treated in vacuum for 1 h at 300°C for the thermal decomposition of $N_2NiO_6 \cdot 6H_2O$ to NiO (Brockner et al., 2007). Subsequently, TGA (TA Instruments Q500) was conducted to determine the NiO loading on the CNT and examine the variations of the oxidation temperature as a function of the NiO content and atmosphere (air and N_2). The samples were analyzed in a platinum pan from room

*Corresponding author. E-mail: cwyang@skku.edu

temperature to 900°C at a heating rate of 5°C/min. Raman spectroscopy (Renishaw RM 1000-In Via) was used to examine the quantity of defects in the CNTs. The *ex situ* heat treatment was conducted at 600°C for 30 min in vacuum or in air. TEM (JEM-2100F, JEOL Co. Ltd.) was employed to observe microstructure of the NiO (50 wt%)/CNT composite. In addition, selected area diffraction (SAD) was used to confirm the phase transition. The *in situ* heating experiments were performed in the TEM (JEM-3011 with a LaB_6 filament operating at 300 keV, JEOL Co. Ltd.). A model EM-21130 JEOL heating holder was used to resistively heat the samples.

Results and Discussion

Figure 1 shows TGA results of the NiO/CNT composite with various NiO contents in air and N_2. Weight losses were observed in each sample and derivative plots were obtained in both atmospheres. The NiO loading after CNT oxidation was confirmed by the weight loss curves in air. The amount of residue remaining increased with increasing NiO loading (see Fig. 1a). On the other hand, in N_2 atmosphere, there was less residue remaining (see Fig. 1b). Derivative plots (DTG) in N_2 revealed peaks at ~540°C (Fig. 1b). In contrast, in air, the peaks were observed at ~400°C with increasing NiO content from 10 to 80 wt% (Fig. 1a). As a reference, the MWCNTs, which were used for this study, were oxidized at ~600°C (data not shown). In other words, NiO affects the oxidation stability and decreases the oxidation temperature of CNT. The main peaks at ~540°C in both atmospheres are believed to have occurred via the same mechanism. Unlike an air atmosphere, which supplies oxygen continuously, in a N_2 atmosphere, there is no oxygen source to oxidize the CNTs except for the oxygen in NiO itself. Therefore, the CNTs were oxidized at the interface between NiO and CNT by consuming oxygen from the NiO and reducing NiO to nickel. This was confirmed by TGA in N_2 atmosphere, which showed less residue with increasing NiO loading (see Fig. 1b). The number of reaction sites that cause CNT oxidation increased with increasing NiO content, and more oxygen could be consumed through CNT oxidation. Consequently, less residue remained in the N_2 atmosphere. In the air atmosphere, however, oxygen vacancies generated by the oxidation of CNT diffuse from the interface between NiO and CNT to the surface of NiO and are regenerated by gas-phase oxygen (Mars & Krevelen, 1954; Aksel & Eder, 2010). Therefore, in air atmosphere, NiO can keep its phase without a transition to nickel, and the amount of residue shown in the TGA results (Fig. 1a) can be understood in the same context.

To confirm and observe the microstructure and phase transition directly through the oxidation of CNT by reducing NiO to nickel, comparative TEM analysis was conducted selectively for the NiO (50 wt%)/CNT composite samples before and after the *ex situ* heat treatment at 600°C for 30 min in vacuum and air atmosphere. Figure 2 shows the TEM results before and after heat treatment. After heating in a vacuum, the phase transition of NiO to nickel was

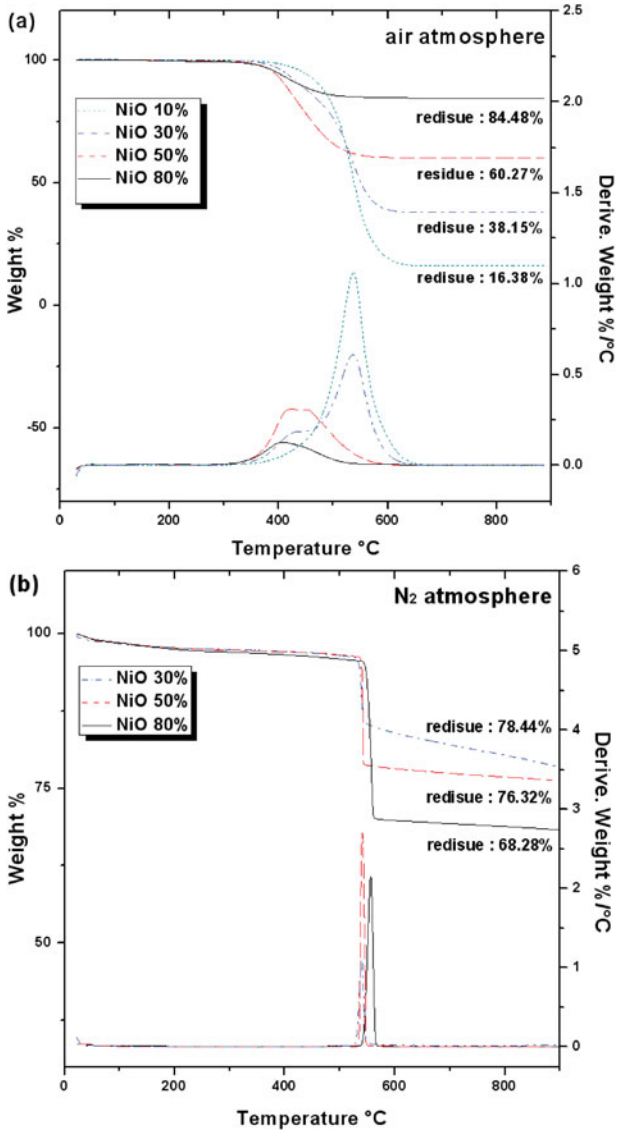

Figure 1. TGA results of NiO/CNT composite with various NiO contents (10, 30, 50, and 80 wt%) in (**a**) air and (**b**) N_2 atmosphere. TGA, thermogravimetric analysis; NiO, nickel oxide; CNT, carbon nanotube.

confirmed by the SAD pattern and fast Fourier transform (FFT) image (Figs. 2b, 2d). During the oxidation of CNT by reducing NiO to nickel in a vacuum, the oxygen in NiO diffuses to the CNT surface and carbon diffuses into nickel because carbon has some solid solubility in nickel (Singleton & Nash, 1989). This was confirmed by the formation of graphitic shell covering the nickel particles, which was formed by the precipitation of supersaturated carbon from nickel with cooling down (Fig. 2b). In contrast, NiO in the sample after heating in air maintains its phase without a transition because reduction by CNT and reoxidation by gaseous O_2 molecules in NiO occur simultaneously (Fig. 2c).

The oxidation mechanism of CNT with reducing NiO can be explained using the Ellingham Diagram. To oxidize CNT, O_2 molecules were adsorbed on the CNT surface first, a C–O bond was formed, and the C–O pair was desorbed

https://doi.org/10.1017/S143192761301266X Published online by Cambridge University Press

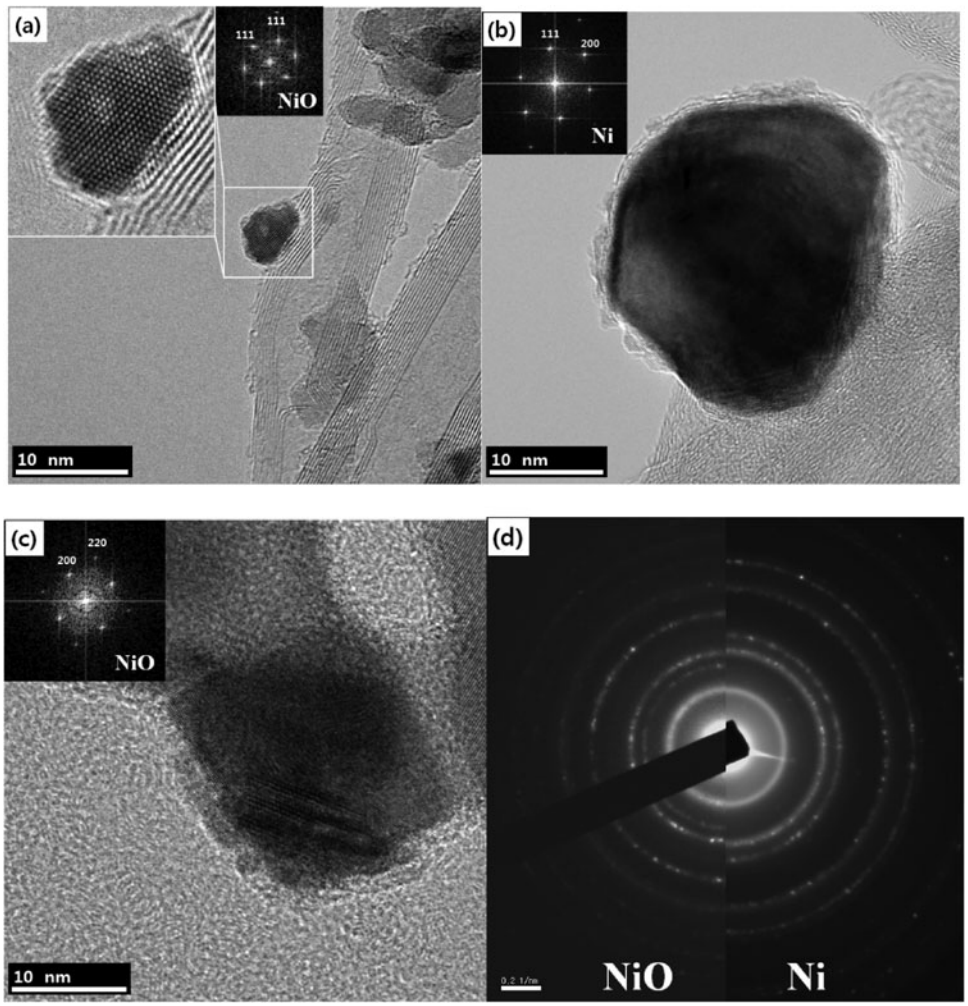

Figure 2. TEM results before and after *ex situ* heat treatment. **a:** NiO particle on CNT before heat treatment. **b:** Nickel particle on CNT after heat treatment in a vacuum. **c:** NiO particle after heat treatment in air. **d:** SAD pattern before and after heat treatment in a vacuum, which shows a phase transition from NiO to nickel. TEM, transmission electron microscopy; NiO, nickel oxide; CNT, carbon nanotube; SAD, selected area diffraction.

with breaking C–C bonds (Zhu et al., 2000; Park et al., 2001). In the Ellingham Diagram, the position of the line for a given reaction shows the stability of the oxide as a function of temperature and can determine the relative ease of reducing a given metallic oxide to metal. Reactions closer to the top of the diagram are the most noble metals, and their oxides are unstable and reduced easily. Toward the bottom of the diagram, the metals become progressively more reactive and their oxides become more difficult to reduce (Ellingham, 1944). To examine the reduction of NiO by CNT, the $2Ni + O_2 \Rightarrow 2NiO$ line and $2C + O_2 \Rightarrow 2CO$ line can be used because a CO molecule was desorbed from the adsorbed phases by breaking the C–C bonds after O_2 adsorption. Both lines are crossed at ~500°C. At temperatures <500°C, the $2C + O_2 \Rightarrow 2CO$ line takes place at the bottom of the $2Ni + O_2 \Rightarrow 2NiO$ line and CNT cannot be oxidized by reducing NiO. On the other hand, at temperatures >500°C, the positions of both lines are reversed and the heat of formation of carbon monoxide is smaller than NiO at ~500°C. Therefore, the main DTG peak at ~540°C in the TGA results in air and N_2 atmospheres with the same mechanism, i.e., because of the oxidation of CNT by consuming oxygen from NiO and generating oxygen vacancies.

On the other hand, with increasing NiO loading (50 and 80 wt%) in air, the peak moved from ~540 to 400°C. This is caused by another mechanism, and is due to defects of CNT, which occur with increasing NiO content. To quantify the increase in defects due to the NiO loading, Raman spectroscopy was carried out with excitation at 633 nm. Figure 3 shows the Raman spectra of the CNTs with various NiO contents. The number of defects can be estimated from the D band in the Raman spectrum. Two characteristic peaks near 1,320 and 1,600 cm^{-1} were observed in the NiO/CNT composites. The former, which is known as the D band, originates from the first-order scattering process of sp^3 carbon by the presence of in-plane substitutional hetero-atoms, vacancies, grain boundaries, or other defects, and by finite size effects; all of these reduce the crystalline symmetry of the quasi-infinite lattice (Brown et al., 2001). The latter, which is known as the G band,

https://doi.org/10.1017/S143192761301266X Published online by Cambridge University Press

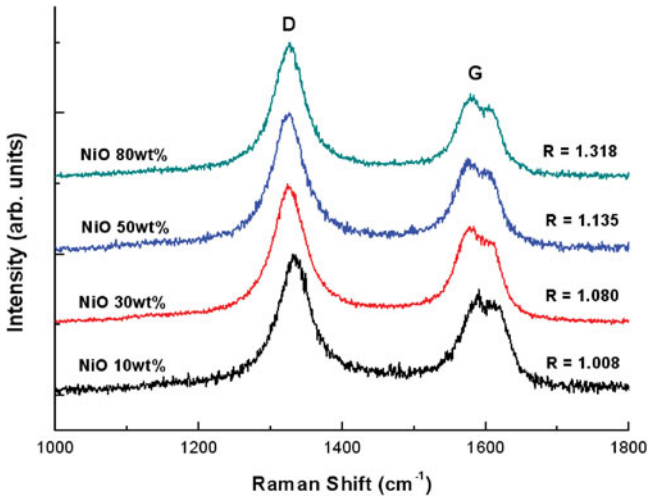

Figure 3. Raman spectra as a function of the NiO loading on CNT. *R* value (the D band/G band ratio) increases with increasing the amount of loading. NiO, nickel oxide; CNT, carbon nanotube.

represents the sp^2 carbon states related to the graphitic hexagon-pinch mode (Osswald et al., 2007). Owing to the origin of the respective bands, the *R* value (i.e., the D band/G band ratio) indicates the quantity of defects (disordered carbon) in the tube walls (Lee et al., 2011). More defects are generated on CNTs with increasing NiO content, which was demonstrated by an increase in *R* value from 1.008 for 10 wt% to 1.318 for 80 wt%. The adsorption energy of an O_2 molecule on defects is much larger than that on a nondefective tube wall. Furthermore, the desorption barriers of the C–O pair from the defects are much lower than those at nondefective wall (Zhu et al., 2000; Park et al., 2001). Therefore, the oxidation rate of disordered carbon and defective tubes by O_2 molecules is much faster than that of the nondefective wall and oxidation occurs at ~400°C (Osswald et al., 2005; Behler et al., 2006).

The temperature when a phase transition occurs was examined directly by observing the dynamic changes in the diffraction patterns of NiO as a function of temperature through an *in situ* heating experiment. Figure 4 shows the *in situ* results. In the SAD patterns, the (200) plane of nickel began to appear at ~500°C, and the (111) and (220) plane of NiO decreased with continued heating. These *ex situ* and *in situ* TEM results are consistent with the TGA results.

Conclusion

This study examined the thermal stability and oxidation mechanism of the NiO/CNT composite. The NiO/CNT composites were prepared by a solution-based method with various NiO contents. The oxidation mechanism was suggested based on the comparative TGA and TEM results in air and N_2 atmosphere and Ellingham Diagram. In addition, phase transitions were observed directly by *in situ* heating TEM. NiO decreases the oxidation temperature of CNTs and acts as a catalyst. CNTs can be oxidized by

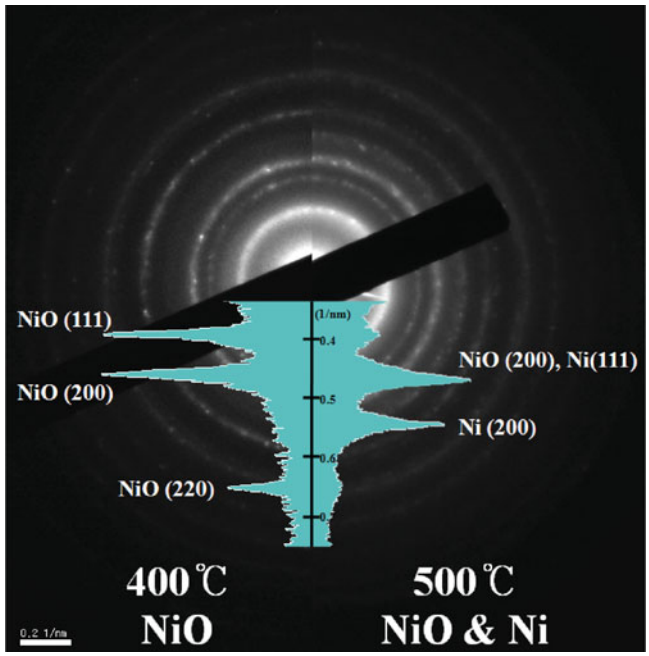

Figure 4. Dynamic change in the SAD patterns during *in situ* heat treatment performed inside TEM. Nickel (200) plane started to appear at ~500°C and NiO (111) and (220) plane decreased with continuous heating. SAD, selected area diffraction; TEM, transmission electron microscopy; NiO, nickel oxide.

reducing NiO to nickel by consuming the oxygen of NiO, even in a N_2 atmosphere. In air, NiO maintains its phase because reduction by CNT and reoxidation by O_2 molecules occur simultaneously. Moreover, with increasing NiO content, the oxidation temperature decreased to much lower temperature because of defects in CNT generated by the NiO loading. The thermal stability of the NiO/CNT composite was examined, and it was affected by NiO and the quantity of defects.

Acknowledgments

This work was supported by the National Research Foundation of Korea (NRF) grants funded by the Korea government (MEST; No. 2011-0017257, No. 2011-0019984, and No. 2011-0030803). The authors gratefully appreciate technical support from the Cooperative Center for Research Facilities (CCRF) at Sungkyunkwan University.

References

Ajayan, P.M., Stephan, O., Redlich, P. & Colliex, C. (1995). Carbon nanotubes as removable templates for metal oxide nanocomposites and nanostructures. *Nature* **375**, 564–567.

Aksel, S. & Eder, D. (2010). Catalytic effect of metal oxides on the oxidation resistance in carbon nanotube-inorganic hybrids. *J Mater Chem* **20**, 9149–9154.

Avouris, P., Chen, Z. & Perebeinos, V. (2007). Carbon-based electronics. *Nat Nanotechnol* **2**, 605–615.

Behler, K., Osswald, S., Ye, H., Dimovski, S. & Gogotsi, Y. (2006). Effect of thermal treatment on the structure of multi-walled carbon nanotubes. *J Nanopart Res* **8**, 615–625.

https://doi.org/10.1017/S143192761301266X Published online by Cambridge University Press

Brockner, W., Ehrhardt, C. & Gjikaj, M. (2007). Thermal decomposition of nickel nitrate hexahydrate, $Ni(NO_3)_2 \cdot 6H_2O$, in comparison to $Co(NO_3)_2 \cdot 6H_2O$ and $Ca(NO_3)_2 \cdot 6H_2O$. *Thermochim Acta* **456**, 64–68.

Brown, S.D.M., Jorio, A., Dresselhaus, M.S. & Dresselhaus, G. (2001). Observation of the D-band feature in the Raman spectra of carbon nanotubes. *Phys Rev B* **64**, 073403.

Ellingham, H.J.T. (1944). Reducibility of oxides and sulfides in metallurgical processes. *J Soc Chem Ind* **63**, 125–133.

He, K.X., Wu, Q.F., Zhang, X.G. & Wang, X.L. (2006). Electrodeposition of nickel and cobalt mixed oxide/carbon nanotube thin films and their charge storage properties. *J Electrochem Soc* **153**(8), 1568–1574.

Iijima, S. (1991). Helical microtubules of graphitic carbon. *Nature* **354**, 56–58.

Lee, Y.I., Park, M.H., Bae, J.H., Lee, S.E., Song, K.W., Kim, T.H., Lee, Y.H. & Yang, C.W. (2011). Loading behavior of Pt nanoparticles on the surface of multiwalled carbon nanotubes having defects formed via microwave treatment. *J Nanosci Nanotechnol* **11**, 479–483.

Li, C., Wang, D., Liang, T., Wang, X., Wu, J., Hu, X. & Liang, J. (2004). Oxidation of multiwalled carbon nanotubes by air: Benefits for electric double layer capacitors. *Powder Technol* **142**, 175–179.

Lota, K., Sierczynska, A. & Lota, G. (2011). Supercapacitors based on nickel oxide/carbon materials composites. *Int J Electrochem* **2011**, 321473.

Mars, P. & Krevelen, D.W. (1954). Oxidations carried out by means of vanadium oxide catalysts. *Chem Eng Sci* **3**, 41–59.

Osswald, S., Flahaut, E., Ye, H. & Gogotsi, Y. (2005). Elimination of D-band in Raman spectra of double-wall carbon nanotubes by oxidation. *Chem Phys Lett* **402**, 422–427.

Osswald, S., Havel, M. & Gogotsi, Y. (2007). Monitoring oxidation of multiwalled carbon nanotubes by Raman spectroscopy. *J Raman Spectrosc* **38**, 728–736.

Park, Y.S., Choi, Y.C., Kim, K.S., Chung, D.S., Bae, D.J., An, K.H., Lim, S.C., Zhu, X.Y. & Lee, Y.H. (2001). High yield purification of multiwalled carbon nanotubes by selective oxidation during thermal annealing. *Carbon* **39**, 655–661.

Singleton, M. & Nash, P. (1989). The C-Ni (carbon-nickel) system. *Bulletin of Alloy Phase Diagrams* **10**(2), 121–126.

Wang, D.W., Li, F. & Cheng, H.M. (2008). Hierarchical porous nickel oxide and carbon as electrode materials for asymmetric supercapacitor. *J Power Sources* **185**(2), 1563–1568.

Xia, X.H., Tu, J.P., Zhang, J., Wang, X.L., Zhang, W.K. & Huang, H. (2008). Electrochromic properties of porous NiO thin films prepared by a chemical bath deposition. *Sol Energy Mater Sol Cells* **92**(6), 628–633.

Zhu, X.Y., Lee, S.M., Lee, Y.H. & Frauenheim, T. (2000). Adsorption and desorption of an O_2 molecule on carbon nanotubes. *Phys Rev Lett* **85**(13), 2757–2760.

https://doi.org/10.1017/S143192761301266X Published online by Cambridge University Press